frontiers in Physics

ORIGINAL RESEARCH
published: 22 September 2021
doi: 10.3389/fphy.2021.752081

Engineering Entangled Photons for Transmission in Ring-Core Optical Fibers

G. Cañas[1], *E. S. Gómez*[2,3], *E. Baradit*[1], *G. Lima*[2,3] *and S. P. Walborn*[2,3]*

[1]*Departamento de Física, Universidad del Bío-Bío, Concepción, Chile,* [2]*Departamento de Física, Universidad de Concepción, Concepción, Chile,* [3]*Millennium Institute for Research in Optics, Universidad de Concepción, Concepción, Chile*

The capacity of optical communication channels can be increased by space division multiplexing in structured optical fibers. Radial core optical fibers allows for the propagation of twisted light–eigenmodes of orbital angular momentum, which have attracted considerable attention for high-dimensional quantum information. Here we study the generation of entangled photons that are tailor-made for coupling into ring core optical fibers. We show that the coupling of photon pairs produced by parametric down-conversion can be increased by close to a factor of three by pumping the non-linear crystal with a perfect vortex mode with orbital angular momentum ℓ, rather than a gaussian mode. Moreover, the two-photon orbital angular momentum spectrum has a nearly constant shape. This provides an interesting scenario for quantum state engineering, as pumping the crystal with a superposition of perfect vortex modes can be used in conjunction with the mode filtering properties of the ring core fiber to produce simple and interesting quantum states.

Keywords: parametric down conversion, ring-core fiber, entangled photons, orbital angular momentum, perfect vortex beam

OPEN ACCESS

Edited by:
Bao-Sen Shi,
University of Science and Technology of China, China

Reviewed by:
Jianming Wen,
Kennesaw State University, United States
Bi-Heng Liu,
University of Science and Technology of China, China
Mingtao Cao,
National Time Service Center (CAS), China

***Correspondence:**
S. P. Walborn
swalborn@udec.cl

Specialty section:
This article was submitted to Optics and Photonics, a section of the journal Frontiers in Physics

Received: *02 August 2021*
Accepted: *07 September 2021*
Published: *22 September 2021*

Citation:
Cañas G, Gómez ES, Baradit E, Lima G and Walborn SP (2021) Engineering Entangled Photons for Transmission in Ring-Core Optical Fibers. Front. Phys. 9:752081. doi: 10.3389/fphy.2021.752081

1 INTRODUCTION

Distribution of photonic entangled states is a cornerstone of future quantum networks. Most likely, this will need to be realized within the same optical infrastructure as standard telecommunications networks. Recent developments in optical fiber technology have resulted in novel fiber core structures, which allow for the propagation of multiple spatial modes. These fibers are expected to play an important role in increasing the transmission capacity of future telecommunications networks through space division multiplexing (SDM) [1]. Examples of SDM fiber candidates include multi-mode fibers [2,3], multi-core fibers [4], and ring core fibers [5], among others. In the quantum regime, SDM technology has attractive features. The multiple spatial modes are a straightforward way to increase the dimension of quantum systems, which has several advantages in quantum key distribution (QKD) [6–11], and have shown to be more resistant to some types of noise [12]. Additional applications can be found in a recent review [13]. In addition to providing multiple channels, it is expected that these fibers will offer more phase stability, when compared to superposition states of several modes propagating in independent fibers [14,15].

Ring-core fibers (RCFs) allow for the propagation of orbital angular momentum (OAM) eigenmodes [16–25], which have attracted considerable attention as they allow for the encoding of high-dimensional quantum information [26–28]. To date, the principal source of entangled photons has been spontaneous parametric down-conversion (SPDC). A beautiful and useful characteristic of SPDC is that the two

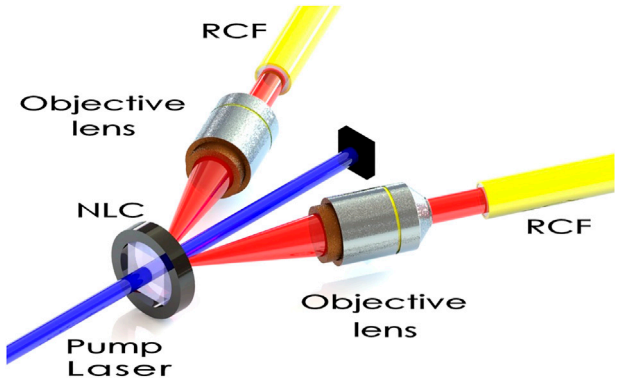

FIGURE 1 | Sketch of the basic idea. SPDC at a thin non-linear crystal (NLC) produces down-converted photon pairs, which are then coupled into ring-core fibers. The angle between the down-converted beams and the pump beam is exaggerated in the Panel for visual clarity. In the calculations, it is assumed to be small enough so that the setup can be treated as co-linear. The optical systems are such that the image plane of the crystal coincides with the entrance face of the fibers, with appropriate magnification factors.

photon spatial state can be engineered by manipulating the pump beam [29–35]. This has led to the production of quantum states with interesting properties [36–40]. The entanglement properties of these states are determined by the mode decomposition of the two-photon state, in which one has the freedom to choose between quite a few families of transverse modes. Of particular interest are those decompositions onto OAM eigen-modes such as Laguerre-Gauss [41–44] or Bessel-Gauss [45–47], which comprise a set of Schmidt modes of the two-photon state [48,49].

In this paper we study the coupling of down-converted photons into RCFs and the two-photon state that is produced, as sketched in **Figure 1**. We consider the decomposition of the two-photon state in terms of perfect vortex (PV) modes, which can have near-perfect fidelity with the eigen-modes of RCFs [25]. We show that by pumping the down-conversion crystal with a PV pump beam, the amplitude of the most relevant down-converted PV modes can be increased while maintaining a high degree of entanglement. While the two-photon OAM mode spectrum is wider for a gaussian pump beam, leading to larger Schmidt numbers, this increase in entanglement is irrelevant when coupling into RCFs or similar optical devices, as only a finite set of lower-order PV modes excite the fiber eigen-modes. In addition, the shape of the mode spectrum is nearly independent of the OAM of the PV pump beam. The combination of the two-photon state engineering using PV pump beams and the mode filtering provided by the RCF can be a powerful tool, providing a simple method to generate interesting two-photon states, some examples of which are discussed in **section 4**.

2 PERFECT VORTEX BEAMS AND RING CORE FIBERS

An illustration of a RCF is shown in **Figure 2**. It is described by a ring-shaped core, with interior radius b and exterior radius a. A set of eigenmodes of the RCF (circularly symmetric LP modes) have an azimuthal phase dependence $e^{i\ell\phi}$, and thus carry OAM [50]. In Ref. 25 it was shown that an example of a commercially available RCF supports 13 LP modes with OAM $\ell = 0, \pm1, \pm2, \cdots \pm 6$. Moreover, depending on the fiber properties, they can have near perfect (~ 0.995) overlap with the so-called PV modes with the same value of ℓ. PV modes are the Fourier transform of Bessel-Gaussian beams, carrying OAM with eigenvalue ℓ. They are given by [51].

$$\mathcal{U}_\ell(\boldsymbol{r}) = N \exp(i\ell\phi) u_\ell(r), \tag{1}$$

where N is a normalization constant and the radial component is given by

$$u_\ell(r) = \exp\left(-\frac{(r^2 + r_r^2)}{w_0^2}\right) I_\ell\left(\frac{2rr_r}{w_0^2}\right), \tag{2}$$

with I_ℓ the modified Bessel function of the first kind. The parameters r_r and w_0 are the ring radius and the Gaussian beam waist at the focus. As shown in Ref. 51, with certain parameter relations, the radial function can be approximated by

$$u_\ell(r) \approx u(r) = \exp\left(-\frac{(r - r_r)^2}{w_0^2}\right), \tag{3}$$

which presents the interesting property that it is independent of ℓ. Numerical evaluation of the overlap between normalized versions of **(2)** and **(3)** is near unity when $\ell \lesssim 3r_r/w_0$. The ring-shape with constant radius makes these modes attractive for coupling into RCFs [25,51–53]. Thus, entangled photons in perfect vortex modes are an interesting candidate for distribution of entanglement in RCFs.

3 SPONTANEOUS PARAMETRIC DOWN-CONVERSION WITH PV MODES

The two-photon state produced from SPDC using a continuous-wave, monochromatic pump beam incident on a thin non-linear crystal, is given by [29,54–56].

$$|\psi\rangle = \iint d\boldsymbol{q}_1 d\boldsymbol{q}_2 \psi(\boldsymbol{q}_1, \boldsymbol{q}_2) |\boldsymbol{q}_1\rangle |\boldsymbol{q}_2\rangle, \tag{4}$$

where $\boldsymbol{q}_l$ ($l = 1, 2$) are transverse components of the down-converted wave vectors. The single photons with transverse wave vector q_l and frequency ω_l are written as $|\boldsymbol{q}_l\rangle$. The two-photon amplitude in the paraxial regime, written in wave vector coordinates at the exit face of the crystal is given by

$$\psi(\boldsymbol{q}_1, \boldsymbol{q}_2) = \mathcal{V}(\boldsymbol{q}_1 + \boldsymbol{q}_2) \mathrm{sinc}[(k_{1z} + k_{2z} - k_{pz})L/2]. \tag{5}$$

Here L is the length of the non-linear crystal and k_{pz} is the z-component of the pump beam wavevector. The function $\mathcal{V}(\boldsymbol{q})$ is the angular spectrum of the pump beam [29], and the sinc function is known as the phase matching function [55]. For simplicity, all modes are assumed to be polarized. If narrowband filters are used to detect the photons, we can assume monochromatic down-converted fields, and apply the Fresnel approximation $k_z \approx k(1 - q^2/2k^2)$, which gives

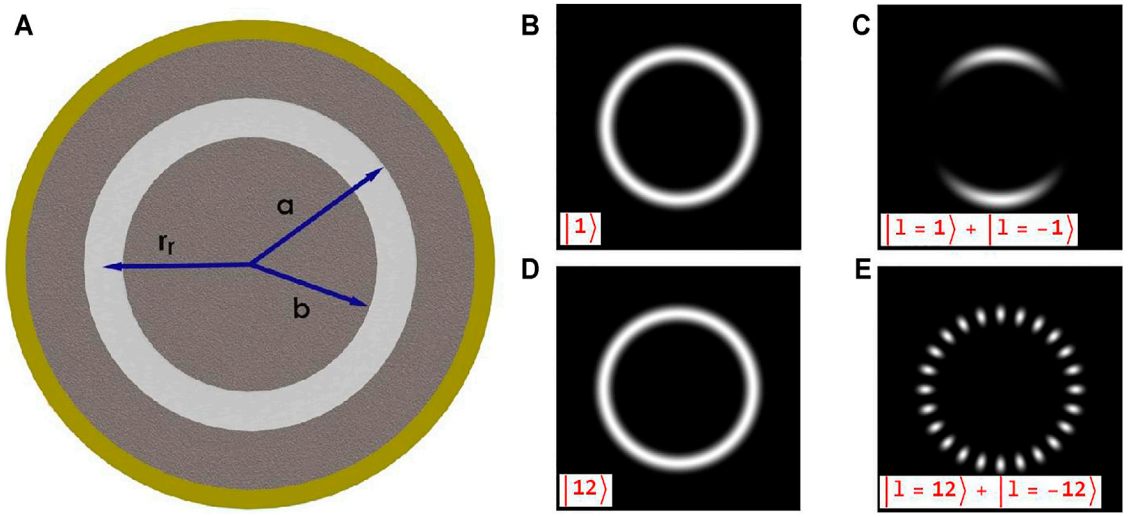

FIGURE 2 | (A) Illustration of a Ring-Core Fiber (RCF). **(B)**, **(D)** Profiles of perfect vortex modes and **(C)**, **(E)** superpositions of perfect vortex modes.

$$k_{1z} + k_{2z} - k_{pz} \approx -\frac{1}{2k_p}[\delta_1 \boldsymbol{q}_1 - \delta_2 \boldsymbol{q}_2]^2, \tag{6}$$

where we define $k_p \equiv |\boldsymbol{k}_p|$ as the wavenumber of the pump beam, and $\delta_1 = \sqrt{k_2/k_1}$, $\delta_2 = \sqrt{k_1/k_2}$. We can rewrite the two-photon amplitude as:

$$\psi(\boldsymbol{q}_1, \boldsymbol{q}_2) = \mathcal{V}(\boldsymbol{q}_1 + \boldsymbol{q}_2)\mathcal{S}\left([\delta_1 \boldsymbol{q}_1 - \delta_2 \boldsymbol{q}_2]^2\right), \tag{7}$$

where $\mathcal{S}(\boldsymbol{q}) = A\text{sinc}\left(Lq^2/4k_p\right)$. Defining the variables

$$\boldsymbol{Q}_\pm = \boldsymbol{q}_1 \pm \boldsymbol{q}_2, \tag{8}$$

$$\boldsymbol{R}_\pm = \frac{1}{2}(\boldsymbol{r}_1 \pm \boldsymbol{r}_2) \tag{9}$$

$$\delta_\pm = \frac{1}{2}(\delta_1 \pm \delta_2), \tag{10}$$

and taking the Fourier transform of **Eq. 7**, the two-photon amplitude can be written in position coordinates $\boldsymbol{r}_1$, $\boldsymbol{r}_2$ as

$$\Psi(\boldsymbol{r}_1, \boldsymbol{r}_2) = \frac{1}{2}\iint d\boldsymbol{Q}_+ d\boldsymbol{Q}_- e^{i\boldsymbol{Q}_+\boldsymbol{R}_+} e^{i\boldsymbol{Q}_-\boldsymbol{R}_-} \mathcal{V}(\boldsymbol{Q}_+) \times \mathcal{S}\left([\delta_+ \boldsymbol{Q}_+ + \delta_- \boldsymbol{Q}_-]^2\right). \tag{11}$$

By integrating **Eq. 11**, we obtain

$$\Psi(\boldsymbol{r}_1, \boldsymbol{r}_2) = \frac{1}{2}\mathcal{W}\left(\boldsymbol{R}_+ - \frac{\delta_+}{\delta_-}\boldsymbol{R}_-\right)\Gamma(\boldsymbol{R}_-), \tag{12}$$

where $\mathcal{W}$ and Γ are the Fourier transforms of the angular spectrum of the pump beam $\mathcal{V}(q)$ and the phase matching function $\mathcal{S}(q)$, respectively.

3.1 Projection Onto PV Modes

The amplitude to project the two-photon state onto a product state of PV modes is given by

$$\mathcal{A}(\ell_1, \ell_2) = \frac{1}{2}\iint d\boldsymbol{r}_1 d\boldsymbol{r}_2 \Gamma\left(\frac{\boldsymbol{r}_1 - \boldsymbol{r}_2}{2}\right)\mathcal{U}^*_{\ell_1}(\boldsymbol{r}_1)\mathcal{U}^*_{\ell_2}(\boldsymbol{r}_2) \times \mathcal{W}\left(\frac{\boldsymbol{r}_1 + \boldsymbol{r}_2}{2} - \frac{\delta_+}{\delta_-}\frac{\boldsymbol{r}_1 - \boldsymbol{r}_2}{2}\right). \tag{13}$$

In the thin crystal approximation, such that $L \ll z_R$, where z_R is the Rayleigh range of the pump beam, we can approximate $\Gamma(\frac{\boldsymbol{r}_1 - \boldsymbol{r}_2}{2}) \approx 2\delta(\boldsymbol{r}_1 - \boldsymbol{r}_2)$, where $\delta(x)$ is the Dirac delta function. The amplitude becomes

$$\boldsymbol{\mathcal{A}}(\ell_1, \ell_2) = \int d\boldsymbol{r}\mathcal{U}^*_{\ell_1}(\boldsymbol{r})\mathcal{U}^*_{\ell_2}(\boldsymbol{r})\mathcal{W}(\boldsymbol{r}). \tag{14}$$

Assuming now that the pump beam is an OAM eigenstate, it can be written as $\mathcal{W}(\boldsymbol{r}) = M\exp(i\ell\phi)w_\ell(r)$, with M a normalization constant. Then, using expression **(1)** for the PV modes, we have

$$\mathcal{A}(\ell_1, \ell_2, \ell) = (N^*)^2 M \int dr\, r u^*_{\ell 1}(r)u^*_{\ell_2}(r)w_\ell(r) \times \int d\phi e^{i\phi(\ell - \ell_1 - \ell_2)}, \tag{15}$$

which leads to

$$\mathcal{A}(\ell_1, \ell_2, \ell) = \delta_{\ell, \ell_1 + \ell_2}(N^*)^2 M' \int dr\, r u^*_{\ell_1}(r)u^*_{\ell_2}(r)w_\ell(r), \tag{16}$$

where $M' = 2\pi M$. The appearance of the Kronecker delta function guarantees that the OAM winding numbers of the down-converted photons are correlated. These OAM correlations are typically observed in OAM mode decompositions of the two photon state, and corresponds to conservation of the orbital angular momentum [41–46,48,49,57].

3.2 Limited OAM Spectra: Optimizing Into RCF Modes

Let us consider now that the OAM spectra of the down-converted photons are limited by the optical system, such as is the case when

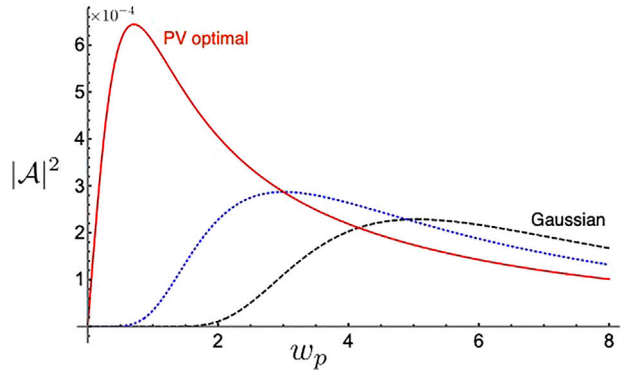

FIGURE 3 | Overlap squared $|\mathcal{A}|^2$ as a function of the pump beam width w_p (in arbitrary units of length) for a gaussian pump beam $r_{rp} = 0$ (black dashed curve), and for a PV pump beam with ring radius $r_{rp} = 2w_0 \approx 0.57r_r$ (blue dotted curve) and ring radius $r_{rp} = r_r = 3.53w_0$ (PV optimal, red solid curve) for best coupling into a commercially available RCF [25]. The optimal PV pump beam increases the probability to produce relevant down-converted modes by a factor of ~ 2.8.

coupling into a RCF, which supports a finite set $\{L\}$ of OAM eigenmodes. We assume that $\ell_j \in \{L\}$ and the ratio r_r/w_0 of the down-converted modes permits approximation of $u_\ell(r) \approx u(r)$, where we recall that this is valid when $\ell_j \lesssim r_r/w_0$. Then, we can write the PV mode product

$$u^*_{\ell_1}(r)u^*_{\ell_2}(r) \approx [u^*(r, r_r, w_0)]^2 = u^*(r, r_r, w_0/\sqrt{2}), \tag{17}$$

where the RCF ring radius and beam width are included explicitly in the argument of these functions for clarity. The integral **(16)** is thus the overlap of a PV radial mode function described by a gaussian ring centered at r_r and ring thickness $w_0/\sqrt{2}$, with the pump radial mode function $w_\ell(r)$. It is thus expected that the amplitude integral is maximized when the pump beam is also a PV beam, with the same ring thickness and ring width. Let us also consider that the pump is prepared in a PV mode and that $w_\ell(r) \approx u(r) \equiv u\ (r, r_{rp}, w_p)$. The amplitude integral **(16)** becomes

$$\mathcal{A} = (N^*)^2 M' \int dr\, r\, u^*(r, r_r, w_0/\sqrt{2})u(r, r_{rp}, w_p), \tag{18}$$

which has the very appealing characteristic that it depends neither on ℓ nor ℓ_1, ℓ_2. In **Figure 3** we show a plot of $|\mathcal{A}|^2$ as a function of the pump beam width w_p for several pump beams, where we used $r_r = 3.53w_0$, corresponding to the parameters of PV modes that are most efficiently coupled into a commercially available RCF [25]. The red solid curve and the blue dotted curve correspond to PV pump beams with ring radii $r_{rp} = r_r$ and $r_{rp} = 2w_0 \approx 0.57r_r$. As a comparison, we also show the squared amplitude when the pump beam is described by a gaussian beam $w(r) = \sqrt{2/(\pi w_p^2)}\exp(-r^2/w_p^2)$. We can see that the amplitude to produce down-converted photons in these eigenmodes can be increased by using a PV pump beam, and reaches a maximum when $w_p = w_0/\sqrt{2}$. In principle, this corresponds to an a factor of ~ 2.8 increase in generation of the relevant down-converted modes. We note that we have considered nearly co-linear SPDC, in which the pump beam and photon pair propagate in the same direction. It has been shown that non-colinear SPDC can lead to asymmetry when the pump beam is a PV mode [58]. Recently, it was shown that the heralding efficiency of a twisted down-converted photon with $\ell_2 = \ell$ (with $\ell_1 = 0$) can be increased by pumping with a PV mode Anwar et al. [47].

An important characteristic here is that, aside from the OAM correlation provided by the Kronecker delta function, the amplitude of the overlap coefficients does not depend upon ℓ_1, ℓ_2 nor ℓ. Thus, considering a post-selected set of PV modes in both the down-converted fields, the two-photon state can be written

$$|\psi\rangle = \frac{\mathcal{A}}{\sqrt{C}} \sum_{\ell-\ell_1,\ell_1 \in \{L\}} |\ell_1\rangle_1 |\ell - \ell_1\rangle_2, \tag{19}$$

where the states $|\ell\rangle$ represent single photon PV modes, i.e., $\langle \boldsymbol{r}|\ell\rangle = \mathcal{U}_\ell(\boldsymbol{r})$, C is a normalization constant, and $\{L\}$ is the set of OAM supported by the fibers. This is a maximally entangled state, whose entanglement depends upon the number of terms in the summation. We emphasize here the fact that **(19)** is valid in the case where the characteristics of the pump and down-converted photons allow the modes to be written in form **(3)**. Typically, this approach is restricted to smaller OAM values. In the next section, we consider the complete two-photon OAM spectrum.

3.3 Unlimited OAM Spectra

When the optical system does not severely limit the OAM spectra of the down-converted photons, such as emission into free space, we can evaluate the amplitude integral **(16)** numerically using **Eq. 2** to describe the modes. Plots of $|\mathcal{A}(\ell_1, \ell - \ell_1, \ell)|^2$ as a function of ℓ_1 are shown in **Figure 4** for $\ell = 0, \pm 3, \pm 12$. To compare the relative weights, we have normalized to the value $|\mathcal{A}(0, 0, 0)|^2$. We can see that the curves have similar forms and magnitudes, but are shifted along the ℓ_1 axis by an amount equal to ℓ.

To compare between a PV and a gaussian pump beam, we evaluated the OAM mode spectra and the entanglement of the two-photon state. **Figure 5A**) shows the normalized probabilites $|\mathcal{A}_{\ell_1}|^2/\sum_{\ell_1}|\mathcal{A}_{\ell_1}|^2$ for a PV pump beam given by **(2)** with the optimal parameters $w_p = w/\sqrt{2}$ and $r_{rp} = r_r = 3.53w_0$, and a gaussian beam with $w_p = 5w$, similar to **section 3.2**. We can see that the probability to produce down-converted PV modes in the range $|\ell_j| \lesssim 15$ ($j = 1, 2$) is larger for the PV pump beam than the gaussian pump beam, and nearly constant for $|\ell_j| \lesssim 6$. Moreover, the probabilities approach zero for $|\ell_j| \sim 30$. The gaussian pump mode, on the other hand, results in an OAM spectrum with much more spread, giving negligible probabilities only when $|\ell_j| \gtrsim 100$ (not shown). The narrower mode spectrum produced by the PV pump beam concentrates the probability in a smaller group of OAM modes, leading to better efficiency when one is working within this finite subspace. For example, looking at the subset of modes corresponding to $|\ell| \leq 15$ (a 31×31 dimensional bipartite system) in **Figure 5A**, this corresponds to 81% of the state produced with the PV pump beam, and only 41% percent of the state produced by the gaussian pump beam. Likewise, for

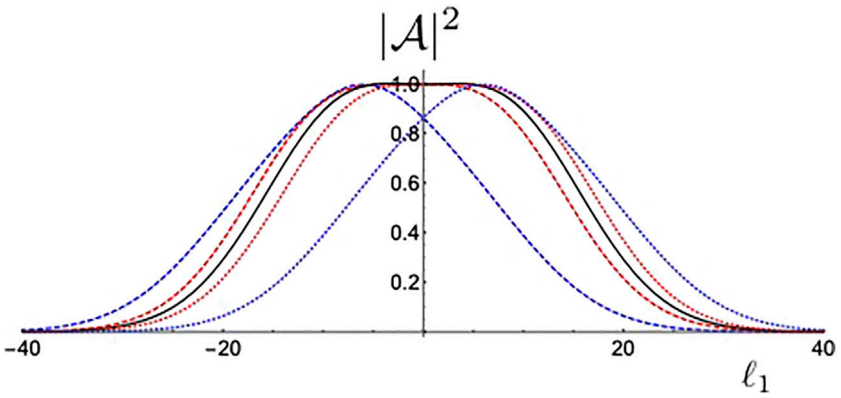

FIGURE 4 | Mode probabilities $|\mathcal{A}(\ell_1, \ell - \ell_1, \ell)|^2$, normalized by $|\mathcal{A}(0,0,0)|^2$, as a function of ℓ_1 for a PV pump beams with optimal width $w_p = w_0/\sqrt{2}$ and ring radius $r_{rp} = r_r$, and OAM number $\ell = 0$ (black solid line), $\ell = \pm 3$ (red dashed and dotted lines) and $\ell = \pm 12$ (blue dashed and dotted lines). The curves are centered at $\ell_1 = \ell$.

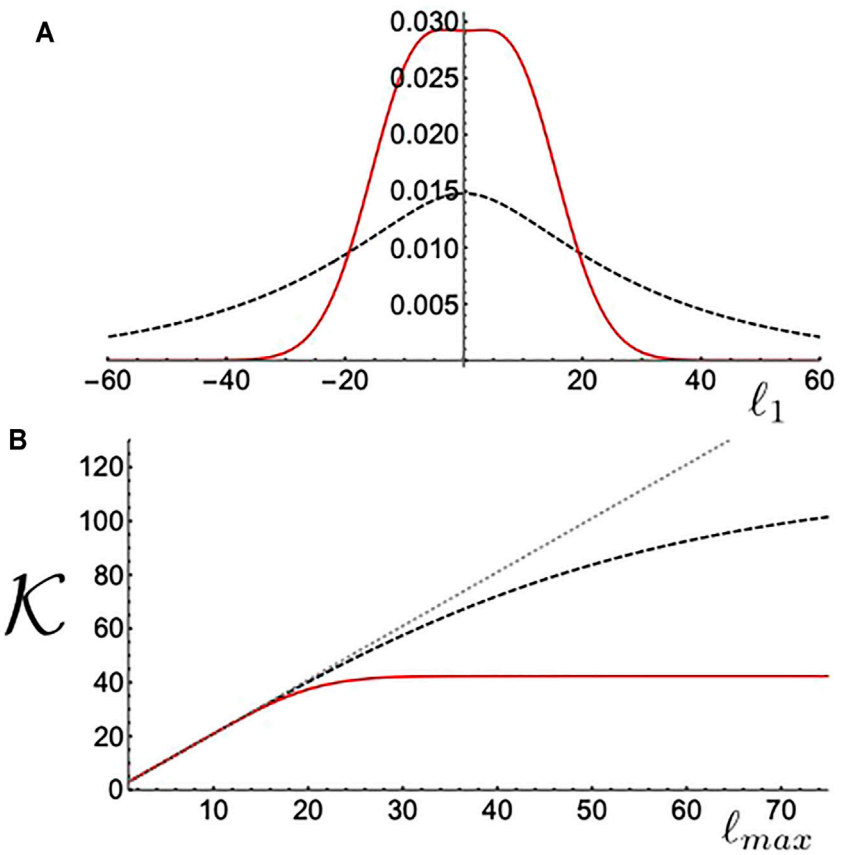

FIGURE 5 | (A) Normalized probabilities for an optimal PV pump beam with $\ell = 0$ (red solid line) and a gaussian pump beam with $w_p = 5w_0$ (black dashed line). The PV pump mode concentrates the probability in lower OAM modes. **(B)** The Schmidt number $\mathcal{K}$ for the two photon state, truncated at $\pm\, \ell_{max}$ for the same pump beams. The grey dotted line corresponds to the maximum allowable Schmidt number, given by $d = 2\ell_{max} + 1$.

generating the 13 OAM modes ($|\ell| \leq 6$) of the RCF fiber studied in Ref. 25, the PV pump beam concentrates 38% of the probability in these modes, compared to 19% for the gaussian pump beam.

It is known that SPDC can produce high-dimensional entanglement in transverse spatial modes [13,26–28,36,59]. Let us see how the PV pump beam compares with a gaussian pump beam for high-dimensional entanglement generation. The

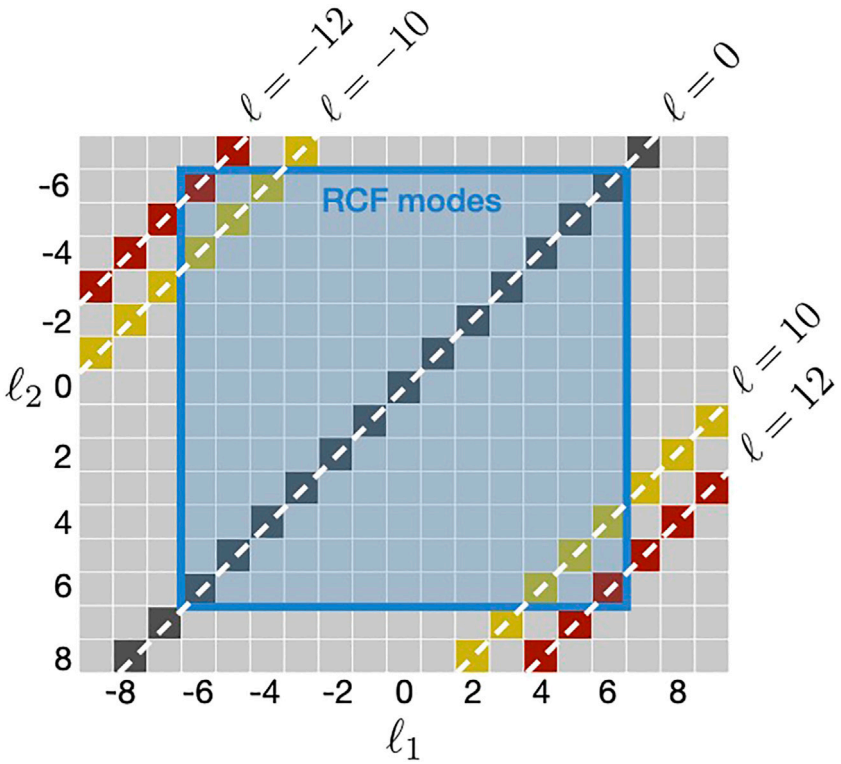

FIGURE 6 | Illustration of state engineering using OAM correlations from SPDC and mode filtering provided by ring core fibers (RCF). OAM correlations between the pump beam and down-converted photons produce photons with OAM distributed along the diagonal directions. The RCF selects modes within the shaded blue square. Thus, only OAM mode pairs along the diagonals within the square will propagate.

entanglement in PV modes can be evaluated by calculating the Schmidt number, given by

$$\mathcal{K} = \frac{\left(\sum_{\ell_1=-\ell_{max}}^{\ell_{max}} \mathcal{A}_{\ell_1}\right)^2}{\sum_{\ell_1=-\ell_{max}}^{\ell_{max}} \mathcal{A}_{\ell_1}^2}, \tag{20}$$

where we assume that the relevant OAM spectrum is limited by $\pm \ell_{max}$, so that the overall dimension of the system is $d = 2\ell_{max} + 1$. In **Figure 5B** we calculate $\mathcal{K}$ for different values of ℓ_{max} for the same pump beams as in **Figure 5A**. The dotted grey line shows the maximum allowable $\mathcal{K} = d$ for comparison. We can see that the PV pump beam results in a Schmidt number that saturates at around $\mathcal{K} \sim 42$, while the gaussian pump beam saturates at $\mathcal{K} \sim 128$ for $\ell_{max} \sim 150$ (not shown). For smaller values of ℓ_{max}, the PV beam and gaussian beam give almost equivalent Schmidt number, and nearly saturate the maximum allowed value of d. We also calculated the largest Schmidt numbers for PV pump modes with $|\ell| \leq 12$, and obtained nearly constant results in the range $\mathcal{K} \sim 40 - 43$. Thus, if the optical system imposes no practical limit on the system dimension, the Gaussian beam allows for higher-dimensional entanglement. Nonetheless, for the more realistic scenario in which the optical system supports a finite set of modes with smaller values of $|\ell_j|$, a PV pump beam concentrates the probability into a smaller set of modes, resulting in a more efficient source, and near maximal entanglement.

4 APPLICATION TO QUANTUM STATE ENGINEERING

Engineering of quantum states with different properties is both a challenge and a goal in quantum information science. In SPDC, this can be achieved by manipulation of the properties of the pump beam, as well as through mode filtering of the individual photons. In this regard, integrating the SPDC results from the last sections together with the transmission properties of RCFs presents several interesting possibilities.

As shown in **Figures 4**, **5**, the PV pump mode concentrates the two-photon probability into a smaller set of joint OAM modes, which is particularly interesting when the photons are coupled into devices that support a finite number of eigen-modes. Let us consider that both down-converted photons are coupled to RCFs that support OAM eigenmodes with $|\ell_1|, |\ell_2| \leq 6$, as was studied in Ref. 25. Thus, each down-converted photon has an OAM spectrum that is truncated in the shaded blue square region shown in **Figure 6**. When the pump beam is described by a single PV mode with OAM ℓ, the two-photon state is described by **(19)**. The important point here is that the state **(19)** contains joint OAM modes with $\ell_2 = \ell - \ell_1$, non-zero overlap integral **(18)**, and

with $|\ell_1|, |\ell_2| \leq 6$. These three conditions can be used to engineer the quantum state. **Figure 6** illustrates the allowable joint OAM spectra for different pump beams, where allowed mode combinations appear on the diagonals, as a function of the pump OAM number ℓ, and within the blue square region, corresponding to the mode selection of the RCF. Since for this set of modes the overlap integral is approximately given by **(18)**, which is independent of the OAM of the pump and down-converted fields, the pump OAM ℓ can be used as a parameter to control the entanglement, where the Schmidt number of the state is essentially determined by the number of OAM components distributed along diagonals and within the RCF square. Thus, one can achieve a 13-dimensional entangled state by pumping with $\ell = 0$. Alternatively, a separable product state can be achieved by pumping with $\ell = \pm 12$, which gives a two-photon state $|\psi\rangle = |\pm 6\rangle_1 |\pm 6\rangle_2$, since these are the only joint OAM modes that are both produced in SPDC and supported by the RCF.

A maximally entangled pair of qubits is arguably the most useful quantum state, with numerous applications in quantum information, such as teleportation and quantum key distribution. This state can be created by using a pump beam that is a superposition of PV modes. For example, using a pump beam described by a PV mode superposition $\mathcal{E}(\boldsymbol{r}) = \alpha \mathcal{U}_{12}(\boldsymbol{r}) + \beta \mathcal{U}_{-12}(\boldsymbol{r})$, with intensity profile illustrated in **Figure 2E**, the two-photon state that propagates in the RCFs modes is

$$|\psi_{\pm 12}\rangle = \alpha |6\rangle_1 |6\rangle_2 + \beta |-6\rangle_1 |-6\rangle_2. \tag{21}$$

Maximal entanglement is achieved when $|\alpha| = |\beta|$. Similar Bell-type states have been prepared in OAM modes from SPDC, however, they rely on post-selection at the detection system [57,60]. Moreover, we note that here the OAM numbers are correlated ($\ell_1 = \ell_2$), as opposed to anti-correlated ($\ell_1 = -\ell_2$), as is usually the case due to OAM conservation. Correlated OAM states have been shown to be useful for quantum metrology [61].

By the same rationale, pumping with an equally weighted superposition of ±10, we have

$$|\psi_{\pm 10}\rangle = \frac{1}{\sqrt{6}} (|4\rangle_1 |6\rangle_2 + |5\rangle_1 |5\rangle_2 + |6\rangle_1 |4\rangle_2 + |-4\rangle_1 |-6\rangle_2 + |-5\rangle_1 |-5\rangle_2 + |-6\rangle_1 |-4\rangle_2), \tag{22}$$

which is a 6 × 6 maximally entangled state. Higher-dimensional states can provide higher key transmission rates in quantum key distribution [6–11], as well as increased resilience to noise [12] and other applications [13,27,28]. These are just a few simple examples of how the dimension and entanglement of the two-photon state can be controlled by manipulating the PV pump beam and post-selection capabilities of the ring-core fiber. More complex quantum states can be created by considering different linear combinations of PV pump beams.

5 CONCLUSION

The generation of entangled photons in perfect vortex modes was studied in the spontaneous parametric down-conversion process. Perfect vortex modes carry orbital angular momentum, and have very high fidelity with the eigen-modes of ring-core optical fibers. We show that pumping the non-linear crystal with a perfect-vortex beam, leads to an output two-photon state that is concentrated in a smaller set of modes, when compared to that of a Gaussian pump beam. It is shown that a near three-fold increase in the coupling efficiency into ring-core fibers could be achieved. Moreover, the two-photon mode spectrum can have near constant magnitude, allowing for a high degree of entanglement.

The use of ring-core fibers as mode filters together with pump beam engineering can be a powerful tool for crafting novel quantum states. Several examples are given, ranging from product states to 13 × 13 dimensional entangled states. These can be produced by changing a single pump beam parameter. Though we focus only on OAM modes, our findings can be combined with correlations in other degrees of freedom, such as polarization. We expect our results will be important for integrating entangled photon sources with future optical fiber networks that employ structured optical fibers.

DATA AVAILABILITY STATEMENT

The original contributions presented in the study are included in the article/Supplementary Material, further inquiries can be directed to the corresponding author.

AUTHOR CONTRIBUTIONS

GC, EG, EB, GL, and SW conceived the work, GC and SW performed the calculations, all authors analyzed results and wrote the manuscript.

FUNDING

This work was supported by the Chilean agencies Fondo Nacional de Desarrollo Científico y Tecnológico (FONDECYT) (1190933, 1190901, 1200266, 1200859) and ANID–Millennium Science Initiative Program–ICN17_012.

ACKNOWLEDGMENTS

The authors thank S. E. Restrepo for valuable discussions.

REFERENCES

1. Richardson DJ, Fini JM, and Nelson LE. Space-division Multiplexing in Optical Fibres. *Nat Photon* (2013) 7:354–62. doi:10.1038/nphoton.2013.94
2. Sillard P, Bigot-Astruc M, and Molin D. Few-mode Fibers for Mode-Division-Multiplexed Systems. *J Lightwave Technol* (2014) 32:2824–9. doi:10.1109/jlt.2014.2312845
3. Rademacher G, Luís RS, Puttnam BJ, Eriksson TA, Ryf R, Agrell E, et al. High Capacity Transmission with Few-Mode Fibers. *J Lightwave Technol* (2019) 37:425–32. doi:10.1109/jlt.2018.2870038
4. Saitoh K, and Matsuo S. Multicore Fiber Technology. *J Lightwave Technol* (2016) 34:55–66. doi:10.1109/jlt.2015.2466444
5. Brunet C, Ung B, Wang L, Messaddeq Y, LaRochelle S, and Rusch LA. Design of a Family of Ring-Core Fibers for OAM Transmission Studies. *Opt Express* (2015) 23:10553–63. doi:10.1364/OE.23.010553
6. Bourennane M, Karlsson A, and Bjork G. Quantum Key Distribution Using Multilevel Encoding. *Phys Rev A (Atomic, Mol Opt Physics)* (2001) 64:012306. doi:10.1103/physreva.64.012306
7. Collins D, Gisin N, Linden N, Massar S, and Popescu S. *Phys Rev Lett* (2002) 88:040404. doi:10.1103/physrevlett.88.040404
8. Cerf NJ, Bourennane M, Karlsson A, and Gisin N. Security of Quantum Key Distribution Usingd-Level Systems. *Phys Rev Lett* (2002) 88:127902. doi:10.1103/physrevlett.88.127902
9. Walborn SP, Lemelle DS, Almeida MP, and Ribeiro PH. Quantum Key Distribution with Higher-Order Alphabets Using Spatially Encoded Qudits. *Phys Rev Lett* (2006) 96:090501. doi:10.1103/PhysRevLett.96.090501
10. Huber M, and Pawłowski M. Weak Randomness in Device-independent Quantum Key Distribution and the Advantage of Using High-Dimensional Entanglement. *Phys Rev A* (2013) 88:032309. doi:10.1103/PhysRevA.88.032309
11. Cañas G, Vera N, Cariñe J, González P, Cardenas J, Connolly PWR, et al. High-dimensional Decoy-State Quantum Key Distribution over Multicore Telecommunication Fibers. *Phys Rev A* (2017) 96:022317. doi:10.1103/physreva.96.022317
12. Zhu F, Tyler M, Valencia NH, Malik M, and Leach J. Is High-Dimensional Photonic Entanglement Robust to Noise? *AVS Quan Sci* (2021) 3:011401. doi:10.1116/5.0033889
13. Erhard M, Krenn M, and Zeilinger A. Advances in High-Dimensional Quantum Entanglement. *Nat Rev Phys* (2020) 2:365–81. doi:10.1038/s42254-020-0193-5
14. Ding Y, Bacco D, Dalgaard K, Cai X, Zhou X, Rottwitt K, et al. High-dimensional Quantum Key Distribution Based on Multicore Fiber Using Silicon Photonic Integrated Circuits. *Npj Quan Inf* (2017) 3:25. doi:10.1038/s41534-017-0026-2
15. Xavier GB, and Lima G. Quantum Information Processing with Space-Division Multiplexing Optical Fibres. *Commun Phys* (2020) 3:9. doi:10.1038/s42005-019-0269-7
16. Bozinovic N, Yue Y, Ren Y, Tur M, Kristensen P, Huang H, et al.Terabit-scale Orbital Angular Momentum Mode Division Multiplexing in Fibers. *Science* (2013) 340:1545–8. doi:10.1126/science.1237861
17. Nejad RM, Allahverdyan K, Vaity P, Amiralizadeh S, Brunet C, Messaddeq Y, et al.Mode Division Multiplexing Using Orbital Angular Momentum Modes over 1.4-km Ring Core Fiber. *J Lightwave Technol* (2016) 34:4252–8. doi:10.1109/jlt.2016.2594698
18. Gregg P, Kristensen P, and Ramachandran S. Conservation of Orbital Angular Momentum in Air-Core Optical Fibers. *Optica* (2015) 2:267–70. doi:10.1364/optica.2.000267
19. Ramachandran S, Gregg P, Kristensen P, and Golowich SE. On the Scalability of Ring Fiber Designs for Oam Multiplexing. *Opt Express* (2015) 23:3721–30. doi:10.1364/oe.23.003721
20. Gregg P, Kristensen P, and Ramachandran S. 134km OAM State Propagation by Recirculating Fiber Loop. *Opt Express* (2016) 24:18938–47. doi:10.1364/oe.24.018938
21. Zhu L, Zhu G, Wang A, Wang L, Ai J, Chen S, et al. 18 Km Low-Crosstalk OAM + WDM Transmission with 224 Individual Channels Enabled by a Ring-Core Fiber with Large High-Order Mode Group Separation. *Opt Lett* (2018) 43:1890–3. doi:10.1364/OL.43.001890
22. Zhu G, Hu Z, Wu X, Du C, Luo W, Chen Y, et al. Scalable Mode Division Multiplexed Transmission over a 10-km Ring-Core Fiber Using High-Order Orbital Angular Momentum Modes. *Opt Express* (2018) 26:594–604. doi:10.1364/oe.26.000594
23. Cozzolino D, Bacco D, Da Lio B, Ingerslev K, Ding Y, Dalgaard K, et al. Orbital Angular Momentum States Enabling Fiber-Based High-Dimensional Quantum Communication. *Phys Rev Appl* (2019) 11:064058. doi:10.1103/physrevapplied.11.064058
24. Zhang J, Liu J, Shen L, Zhang L, Luo J, Liu J, et al.Mode-division Multiplexed Transmission of Wavelength-Division Multiplexing Signals over a 100-km Single-Span Orbital Angular Momentum Fiber. *Photon Res* (2020) 8:1236–42. doi:10.1364/prj.394864
25. Rojas-Rojas S, Cañas G, Saavedra G, Gómez ES, Walborn SP, and Lima G. Evaluating the Coupling Efficiency of Oam Beams into Ring-Core Optical Fibers. *Opt Express* (2021) 29:23381–92. doi:10.1364/OE.425419
26. Bavaresco J, Herrera Valencia N, Klöckl C, Pivoluska M, Erker P, Friis N, et al.Measurements in Two Bases Are Sufficient for Certifying High-Dimensional Entanglement. *Nat Phys* (2018) 14:1032–7. doi:10.1038/s41567-018-0203-z
27. Erhard M, Fickler R, Krenn M, and Zeilinger A. Twisted Photons: New Quantum Perspectives in High Dimensions. *Light Sci Appl* (2018) 7:17146. doi:10.1038/lsa.2017.146
28. Forbes A, and Nape I. Quantum Mechanics with Patterns of Light: Progress in High Dimensional and Multidimensional Entanglement with Structured Light. *AVS Quan Sci* (2019) 1:011701. doi:10.1116/1.5112027
29. Monken CH, Ribeiro PHS, and Pádua S. Transfer of Angular Spectrum and Image Formation in Spontaneous Parametric Down-Conversion. *Phys Rev A* (1998) 57:3123–6. doi:10.1103/physreva.57.3123
30. Torres JP, Deyanova Y, Torner L, and Molina-Terriza G. Preparation of Engineered Two-Photon Entangled States for Multidimensional Quantum Information. *Phys Rev A* (2003) 67:052313. doi:10.1103/physreva.67.052313
31. Miatto FM, Yao AM, and Barnett SM. Full Characterization of the Quantum Spiral Bandwidth of Entangled Biphotons. *Phys Rev A* (2011) 83:033816. doi:10.1103/physreva.83.033816
32. Yao AM. Angular Momentum Decomposition of Entangled Photons with an Arbitrary Pump. *New J Phys* (2011) 13:053048. doi:10.1088/1367-2630
33. Kovlakov EV, Bobrov IB, Straupe SS, and Kulik SP. Spatial bell-state Generation without Transverse Mode Subspace Postselection. *Phys Rev Lett* (2017) 118:030503. doi:10.1103/PhysRevLett.118.030503
34. Liu S, Zhou Z, Liu S, Li Y, Li Y, Yang C, et al.Coherent Manipulation of a Three-Dimensional Maximally Entangled State. *Phys Rev A* (2018) 98:062316. doi:10.1103/PhysRevA.98.062316
35. Kovlakov EV, Straupe SS, and Kulik SP. Quantum State Engineering with Twisted Photons via Adaptive Shaping of the Pump Beam. *Phys Rev A* (2018) 98:060301. doi:10.1103/PhysRevA.98.060301
36. Walborn SP, and Monken CH. Transverse Spatial Entanglement in Parametric Down-Conversion. *Phys Rev A* (2007) 76:062305. doi:10.1103/physreva.76.062305
37. Nogueira WA, Walborn SP, Pádua S, and Monken CH. Generation of a Two-Photon Singlet Beam. *Phys Rev Lett* (2004) 92:043602. doi:10.1103/PhysRevLett.92.043602
38. Vicuña Hernández V, Santiago JT, Jerónimo-Moreno Y, Ramírez-Alarcón R, Cruz-Ramírez H, U'Ren AB, et al. Double Transverse Wave-Vector Correlations in Photon Pairs Generated by Spontaneous Parametric Down-Conversion Pumped by Bessel-Gauss Beams. *Phys Rev A* (2016) 94:063863.
39. Gutiérrez-López D, Maldonado-Terrón M, Hernández RJ, Vicuña-Hernández V, Ramírez-Alarcón R, Cruz-Ramírez H, et al. Spatial Control of Spontaneous Parametric Down-Conversion Photon Pairs through the Use of Apertured Bessel-Gauss Pump Beams. *Phys Rev A* (2019) 100:013802. doi:10.1103/PhysRevA.100.013802
40. Baghdasaryan B, and Fritzsche S. Enhanced Entanglement from Ince-Gaussian Pump Beams in Spontaneous Parametric Down-Conversion. *Phys Rev A* (2020) 102:052412. doi:10.1103/PhysRevA.102.052412
41. Arnaut HH, and Barbosa GA. *Phys Rev Lett* (2001) 85:286.
42. Franke-Arnold S, Barnett SM, Padgett MJ, and Allen L. Two-photon Entanglement of Orbital Angular Momentum States. *Phys Rev A* (2002) 65:033823. doi:10.1103/physreva.65.033823
43. Torres JP, Alexandrescu A, and Torner L. Quantum Spiral Bandwidth of Entangled Two-Photon States. *Phys Rev A* (2003) 68:050301. doi:10.1103/physreva.68.050301

44. Walborn SP, de Oliveira AN, Thebaldi RS, and Monken CH. Entanglement and Conservation of Orbital Angular Momentum in Spontaneous Parametric Down-Conversion. *Phys Rev A* (2004) 69:023811. doi:10.1103/physreva.69.023811
45. McLaren M, Agnew M, Leach J, Roux FS, Padgett MJ, Boyd RW, et al.Entangled Bessel-Gaussian Beams. *Opt Express* (2012) 20:23589–97. 10.1364/OE.20.023589.
46. McLaren M, Romero J, Padgett MJ, Roux FS, and Forbes A. Two-photon Optics of Bessel-Gaussian Modes. *Phys Rev A* (2013) 88:033818. doi:10.1103/PhysRevA.88.033818
47. Anwar A, Prabhakar S, and Singh RP. Size Invariant Twisted Optical Modes for Efficient Generation of Higher Dimensional Quantum States (2021). Available at: https://www.osapublishing.org/josab/upcoming_pdf.cfm?id=436088 (Accessed August 17, 2021).
48. Law CK, and Eberly JH. Analysis and Interpretation of High Transverse Entanglement in Optical Parametric Down Conversion. *Phys Rev Lett* (2004) 92:127903. doi:10.1103/physrevlett.92.127903
49. Straupe SS, Ivanov DP, Kalinkin AA, Bobrov IB, and Kulik SP. Angular Schmidt Modes in Spontaneous Parametric Down-Conversion. *Phys Rev A* (2011) 83. doi:10.1103/PhysRevA.83.060302
50. Allen L, Beijersbergen MW, Spreeuw RJC, and Woerdman JP. Orbital Angular Momentum of Light and the Transformation of Laguerre-Gaussian Laser Modes. *Phys Rev A* (1992) 45:8185–9. doi:10.1103/physreva.45.8185
51. Vaity P, and Rusch L. Perfect Vortex Beam: Fourier Transformation of a Bessel Beam. *Opt Lett* (2015) 40:597–600. doi:10.1364/OL.40.000597
52. Brunet C, Vaity P, Messaddeq Y, LaRochelle S, and Rusch LA. Design, Fabrication and Validation of an Oam Fiber Supporting 36 States. *Opt Express* (2014) 22:26117–27. doi:10.1364/OE.22.026117
53. Vaity P, Brunet C, Messaddeq Y, LaRochelle S, and Rusch LA. Exciting Oam Modes in Annular-Core Fibers via Perfect Oam Beams. The European Conference on Optical Communication. Bordeaux, France. Cannes, France: ECOC (2014). p. 1–3. doi:10.1109/ECOC.2014.6964195
54. Hong CK, and Mandel L. Theory of Parametric Frequency Down Conversion of Light. *Phys Rev A* (1985) 31:2409–18. doi:10.1103/physreva.31.2409
55. Walborn SP, Monken CH, Pádua S, and Souto Ribeiro PH. Spatial Correlations in Parametric Down-Conversion. *Phys Rep* (2010) 495:87–139. doi:10.1016/j.physrep.2010.06.003
56. Schneeloch J, and Howell JC. Introduction to the Transverse Spatial Correlations in Spontaneous Parametric Down-Conversion through the Biphoton Birth Zone. *J Opt* (2016) 18:053501. doi:10.1088/2040-8978/18/5/053501
57. Mair A, Vaziri A, Weihs G, and Zeilinger A. Entanglement of the Orbital Angular Momentum States of Photons. *Nature* (2001) 412:313–6. doi:10.1038/35085529
58. Jabir MV, Apurv Chaitanya N, Aadhi A, and Samanta GK. Generation of "perfect" Vortex of Variable Size and its Effect in Angular Spectrum of the Down-Converted Photons. *Sci Rep* (2016) 6:21877. doi:10.1038/srep21877
59. Schneeloch J, Tison CC, Fanto ML, Alsing PM, and Howland GA. Quantifying Entanglement in a 68-Billion-Dimensional Quantum State Space. *Nat Commun* (2019) 10:2785. doi:10.1038/s41467-019-10810-z
60. Langford NK, Dalton RB, Harvey MD, O'Brien JL, Pryde GJ, Gilchrist A, et al. *Phys Rev Lett* (2004) 93:053601. doi:10.1103/physrevlett.93.053601
61. D'Ambrosio V, Spagnolo N, Re LD, Slussarenko S, Li Y, Kwek LC, et al.Photonic Polarization Gears for Ultra-sensitive Angular Measurements. *Nat Commun* (2013) 4:2432.

Conflict of Interest: The authors declare that the research was conducted in the absence of any commercial or financial relationships that could be construed as a potential conflict of interest.

Publisher's Note: All claims expressed in this article are solely those of the authors and do not necessarily represent those of their affiliated organizations, or those of the publisher, the editors and the reviewers. Any product that may be evaluated in this article, or claim that may be made by its manufacturer, is not guaranteed or endorsed by the publisher.